## Title
Progress in structural studies of telomerase



## Journal
Current Opinion in Structural Biology, 24(1)

## ISSN
0959-440X

## Authors
Miracco, Edward J
Jiang, Jiansen
Cash, Darian D
et al.

## Publication Date
2014-02-01

## DOI
10.1016/j.sbi.2014.01.008

Peer reviewed

Published in final edited form as:
*Curr Opin Struct Biol*. 2014 February ; 0: 115–124. doi:10.1016/j.sbi.2014.01.008.

# Progress in structural studies of telomerase

**Edward J. Miracco**[1], **Jiansen Jiang**[1,2,3], **Darian Cash**[1], and **Juli Feigon**[1,3]

Edward J. Miracco: emiracco@mbi.ucla.edu; Jiansen Jiang: jsjiang@ucla.edu; Darian Cash: dcash@mbi.ucla.edu; Juli Feigon: feigon@mbi.ucla.edu

[1]Department of Chemistry and Biochemistry, University of California Los Angeles, Los Angeles, CA 90095, USA

[2]Department of Microbiology, Immunology and Molecular Genetics, University of California Los Angeles, Los Angeles, California 90095, USA

[3]California Nanosystems Institute, University of California Los Angeles, Los Angeles, California 90095, USA

## Abstract

Telomerase is the ribonucleoprotein (RNP) reverse transcriptase responsible for synthesizing the 3′ ends of linear chromosomes. It plays critical roles in tumorigenesis, cellular aging, and stem cell renewal. The past two years have seen exciting progress in determining telomerase holoenzyme architecture and the structural basis of telomerase activity. Notably, the first electron microscopy structures of telomerase were reported, of the *Tetrahymena thermophila* telomerase holoenzyme and a human telomerase dimer. In addition to new structures of TERT and TER domains, the first structures of telomerase protein domains beyond TERT, and their complexes with TER or telomeric single-stranded DNA, were reported. Together these studies provide the first glimpse into the organization of the proteins and RNA in the telomerase RNP.

## Introduction

The telomerase holoenzyme is a multi-subunit ribonucleoprotein (RNP) primarily responsible for maintaining and elongating the 3′ ends of linear chromosomes. These ends, known as telomeres, contain repeating G-rich DNA that terminate in a 3′ single-stranded overhang and a complex of species-specific proteins (*e.g.*, shelterin in mammals) [1]. Due to the end replication problem, telomeres shorten after each round of cellular division [2], and once eroded past a critical length, telomere shortening results in cellular senescence and, in some cases, apoptosis [3]. Healthy somatic cells do not have active telomerase, whereas the majority of cancer cells do; this dichotomy has made telomerase inhibition an attractive target for the development of anti-cancer drugs [4].

Telomerase holoenzymes are composed of multiple subunits, including the highly conserved catalytic telomerase reverse transcriptase (TERT), the telomerase RNA (TER), and a suite of species-specific proteins. The four domains of TERT include the TERT essential N-terminal (TEN) domain, the TERT RNA binding domain (TRBD), the reverse transcriptase (RT) domain, and the C-terminal extension (CTE) [5]. The domain architecture of TERT is



Correspondence to: Juli Feigon, feigon@mbi.ucla.edu.

similar to other reverse transcriptases [5], with differences arising from the use of an internal template, and the requirement for translocation for processive telomere repeat synthesis and for TER binding, which are provided by the telomerase specific TEN domain and the TRBD [6,7].

TER varies greatly in size between organisms, from 159 nucleotides (nt) in the ciliated protozoan *Tetrahymena thermophila* [8] to over 2,000 nt in the yeast *Candida glabrata* [9]. All TERs identified to date share a core set of conserved motifs, which include a telomere-complementary template, a template boundary element (TBE), and a pseudoknot, usually enclosed by a helix to form a template/pseudoknot (t/PK) domain [10–14]. Additionally, almost all TERs contain a telomerase-stimulating structure (*e.g.*, Stem-Loop 4 in ciliates and CR4/5 in vertebrates) [15]. Vertebrate TERs also contain a small Cajal body RNA (scaRNA) domain that binds H/ACA scaRNA proteins to form a scaRNP and target telomerase to Cajal bodies [16,17].

Due to its importance to human health and longevity, a structural understanding of telomerase function is of enormous interest; however, structural studies have proved remarkably difficult. The low natural abundance of telomerase and a general inability to solubly overexpress the full-length proteins, as well as the lack of a complete characterization of telomerase holoenzyme components, have limited past structural work mainly to individual domains of TERT and TER (reviewed in [5,18,19]). In the past two years exciting progress has been made in determining the architecture of the telomerase holoenzyme and the structural basis of telomerase activity. Two milestone electron microscopy (EM) structures were published, one of human telomerase and the other of the complete *Tetrahymena* telomerase holoenzyme [20,21]. New information on telomerase holoenzyme assembly and function was obtained from structures of domains of telomerase holoenzyme proteins and RNA, including *Tetrahymena* p65 and Teb1 both free and in complex with TER and telomere DNA, respectively [22,23], *Takifugu rubripes* TERT TRBD [24], and yeast *Kluyveromyces lactis* TER pseudoknot [25]. These new structures and what we have learned from them are the focus of this review. Additionally, although not reviewed in detail here, information on how the H/ACA proteins might assemble and interact with the scaRNA domain of vertebrate TER has been obtained from X-ray crystal and solution NMR structures of *S. cerevisiae* H/ACA RNP proteins [26–29].

## Structural Study of Endogenously Assembled *Tetrahymena* Telomerase Holoenzyme by Electron Microscopy

Telomerase and telomeres were first discovered in the ciliated protozoan *Tetrahymena thermophila* [30,31], which fragments its macronuclear genome into ~20,000 mini-chromosomes. *Tetrahymena* requires a relatively large amount of telomerase for telomere maintenance, making it an ideal model organism for studying telomerase structure and function [32]. The proteins of the *Tetrahymena* telomerase holoenzyme were identified by reciprocal affinity pull-down and mass spectrometry to include Teb1 (p82), p75, p65, p50, p45, and p19, in addition to TERT and TER [33–35]. p65 facilitates assembly of TERT with TER, acting as an RNA chaperone and a stable component of the RNP catalytic core TERT-TER-p65 [36–38]. The subunits p75, p45, and p19, which have no identified domains, form a stable sub-complex (7-1-4) that stimulates activity *in vitro* and may be involved in telomerase recruitment to telomeres [39]. Teb1, which is paralogous to replication protein A (RPA1, RPA70 in humans), enhances both activity and processivity *in vitro* likely by anchoring telomere DNA [35,39]. Little was known about p50 prior to the EM structure determination and the functional studies described below.

The negative-strain EM structure of the *Tetrahymena* telomerase holoenzyme was reconstructed at 25 Å [21] using the model-free random conical tilt (RCT) method of 3D reconstruction [40]. Cryoelectron microscopy (cryoEM) images of the holoenzyme were also collected and analyzed, validating the negative-stain EM structure. The holoenzyme is ~500 kDa and has a highly contoured, asymmetric structure with approximate dimensions of 200×150×80 Å (Figures 1a,b). Using telomerase isolated from different strains each bearing a single TAP-tagged protein, the location of the C-terminus (for TERT, p75, p19, Teb1, p65, and p45[41]) or N-terminus (for p50) of the subunits was identified by affinity labeling with Fab bound to the 3×FLAG tag left on after purification. The location of the TER Stem 2, which includes part of the TBE, was identified from a strain of *Tetrahymena* with the sequence of Stem-Loop 2 modified to bind dimeric MS2 coat protein [21,42]. Combining the information from class averages and EM maps of affinity tagged telomerase and of particles lacking one or more subunits, and modeling (described below), the precise boundaries for TERT, p65, Teb1C, and p50 and the general locations of the proteins in the 7-1-4 sub-complex [35] were identified (Figure 1a). The EM model shows that *Tetrahymena* telomerase holoenzyme is a monomer, as previously proposed [43], containing one copy of each protein plus TER. A major finding was that p50 functions structurally as a central hub, contacting the TERT-TER-p65 RNP catalytic core, Teb1C, and 7-1-4. This finding was complemented functionally by activity assays on telomerase holoenzyme reconstituted *in vitro*; notably, the activity stimulation previously attributed directly to Teb1 requires p50 [21].

Using the available crystal structures of TERT from *Tribolium castaneum* [44,45], *Tetrahymena* TERT TRBD [7] and TEN [6] domains, and the C-terminal domain of p65 bound to TER Stem 4 [22], and the NMR structures of TER Loop 4 [46] and Stem-Loop 2 [47], a complete model of the TERT-TER-p65 RNP catalytic core was fit into the EM map (Figure 1b). The TERT model fits well into the central core of the EM map in only one orientation (cross-correlation coefficient of 91%), and a model of p65 bound to Stem-Loop 4 and Stem 1 fit into the U-shaped EM density at the bottom. While details of the RNP catalytic core model remain to be confirmed by high-resolution cryoEM and/or X-ray crystallography, it is remarkably consistent with known biochemical and functional data [48–53]. For example, the TBE and TER Loop 4 contact opposite ends of the TRBD. Loop 4 is near the intersection of the TRBD and CTE domains of TERT, potentially functioning to close the TERT ring [50] (Figure 1b,c) thereby stimulating activity. The functional equivalent of Stem-Loop 4 in vertebrate TER is P6/P6.1, which crosslinks to the same region of the TRBD where Loop 4 is located in the model [50]. The TERT TEN domain and the pseudoknot were placed into the density next to TERT, where they can interact with telomere DNA [54], but their relative locations remain to be definitely defined.

Teb1 has four oligonucleotide/oligosaccharide binding (OB) folds, as described below, but only the structure of the C-terminal domain of Teb1 (Teb1C) was fit into the EM map, because the Teb1 N and A domains were not visible and only weak density was observed for Teb1B. This apparent inherent flexibility of Teb1 agrees with the proteolytic sensitivity and propensity for dissociation seen previously [35]. In the EM structure, 7-1-4 was seen in multiple conformations, rotating as an intact substructure hinged on p50 [21]. Further structural and biochemical studies are required to elucidate the role of 7-1-4 and whether or not its movement is biologically relevant. In the subunit map, p50 appears to contact p45 but not p75 (Figure 1a,b), but recent biochemical studies indicate that p75 is required for recruitment of p19 and p45 to p50 and that this interaction requires only the N-terminal 30 kDa of p50 [41]. This N-terminal 30 kDa is necessary and sufficient for holoenzyme assembly, activity, and processivity. Consistent with this, EM maps from endogenously assembled telomerase containing only the N-terminal 30 kDa of p50 in complete

replacement of full-length p50 appeared identical to the previously reported EM maps [41]. It is likely that only p50-N30 is present in at least some of those particles.

## Structural Basis of Conformational Change in *Tetrahymena* TER Induced by p65

p65 is a LARP7 member of the La related proteins that bind the UUU-3′ ends of RNAP III transcripts using a La module and also function as RNA folding chaperones (Figure 2a) [55]. The C-terminal domain (CTD) of p65 was shown to be necessary and sufficient to induce a structural change in TER Stem-Loop 4 required for hierarchical assembly of p65-TER with TERT using biochemical methods and single molecule FRET [36,38,56,57]. However, sequence alignment of the p65 CTD revealed no known structural modules. Singh and co-workers determined solution NMR and crystal structures of p65 CTD (Figure 2a), which revealed that it is a cryptic atypical RRM with a βαββαβ2βα topology [22]. The RRM contains a 46 amino acid loop between β2 and β3 (hence it was cryptic), which was partially and completely deleted in the NMR solution and X-ray crystal structures, respectively. The atypical RRM features are an extra β42 strand, absence of the RNP1 and RNP2 sequence on β3 and β1, respectively, and an extra helix α3 that lies across the surface of the β-sheet where single-strand nucleotides typically bind. While deletion of the flexible β2-β3 loop had no effect on p65-TER binding or hierarchical assembly with TERT, deletion of the 20 residues at the C-terminus, which are unstructured both in solution and in the crystal structure, dramatically decreased binding and abolished hierarchical assembly. The structure of p65 CTD in complex with Stem 4 revealed that the first 12 of these residues form a helical extension on α3, called α3x (Figure 2a). Based on sequence homology with other La and LARP7 proteins the authors propose that this is a new class of RRM, called xRRM (extended RRM) [58]. TER Stem 4 contains two helices flanking a conserved GA bulge (Figure 2a). In the complex, the xRRM α3x binds across the major groove between the G-C base pairs on either side of the GA bulge and wedges open the base pairs by inserting 3 aromatic residues (Figure 2a). The G and A bases are flipped out and bind in a pocket between helix α3 and the β-sheet, revealing how the RRM can still bind single-stranded nucleotides on its β-sheet face despite the presence of helix α3. The RNA in the complex is bent by 105°, which is the structural change required for hierarchal assembly of p65-TER with TERT (Figure 1c). The structure of the complex, combined with the modeling in the EM map, reveals how p65 facilitates assembly of TER with TERT by positioning Loop 4 in contact with TERT TRBD and CTE.

## *Tetrahymena* Teb1 has Four OB Folds and Binds Telomeric Single-Stranded DNA

The *Tetrahymena* telomerase protein Teb1 (telomerase binding protein 1) subunit is paralogous to RPA70, which has three DNA-binding OB folds that become ordered upon ssDNA binding [59]. Crystal structures of domains A, B, and C of Teb1 were recently solved, revealing all have OB folds (Figure 2b) as predicted [23]. Knock-down of Teb1 in *Tetrahymena* leads to telomere shortening, and *in vitro* addition of recombinantly expressed Teb1 rescued low-processivity endogenously-assembled telomerase [35]. In addition to the crystal structure of the individual Teb1 A, B, and C domains, Zeng and co-workers cocrystalized a construct of Teb1AB, where the 59 residue loop connecting Teb1A and Teb1B domains was deleted (Teb1AΔB), with d[GGGTTGGGGT] (Figure 2b). Sequence specific binding was observed between Teb1A on the concave face—formed by the β-sheet and β42, β3, and β5 and loops 45 and 12—and the 5′GGGT bases via extensive stacking and hydrogen bonding interactions to the Watson-Crick faces. Since no interactions between the 3′ half of the DNA and Teb1B were resolved in the electron density, their proposed

interactions with Teb1B were investigated by mutagenesis [23]. Although by sequence alignment Teb1 is most similar to RPA70, Teb1A and B are structurally more similar to the telomere end-binding protein protection of telomeres 1 (POT1) A and B domains, which also utilizes nucleobase-specific interactions to bind single-stranded telomeric DNA, consistent with its apparent function [59,60].

The C-domain of Teb1 contains an OB-fold lined with basic residues on its concave face, a zinc ribbon motif, and additional α-helices reminiscent of RPA70C (Figure 2b) [35,59]. Although Teb1C does not independently bind DNA, the binding affinity of telomeric DNA to Teb1BC (residues 324–701) is 10-fold higher than to Teb1B alone, and when the basic OB-fold residues of Teb1C are mutated to alanines in Teb1BC, DNA binding affinity, activity, and processivity are all dramatically reduced [23]. This result suggests Teb1C participates in telomere DNA binding in cooperation with Teb1B. Interestingly, deletion of the zinc finger motif did not impact DNA binding but did impact processivity, suggesting the possibility in light of the EM model that the zinc ribbon motif coordinates the protein-protein interaction between Teb1 and TERT and/or p50 [21,41]. So far structures of telomerase holoenzyme and telomere proteins suggest most species have evolved their own proteins for telomerase function and telomere maintenance [1]. The similarities between Teb1 and POT1 hint that a unified theory of telomere and telomerase holoenzyme proteins may exist, but additional structural and genetic work is required.

## Electron Microscopy Structure of Dimeric Human Telomerase

The known stable components of human telomerase holoenzyme include TERT, TER, the H/ACA RNP components dyskerin, Nop10, Gar1, and Nhp2, and the Cajal-body localization protein WDR79/TCAB1 [17]. Canonical H/ACA RNPs function in site-specific pseudouridylation using the internal loops in their RNA subunit as a template [61]. In the case of telomerase, the H/ACA proteins bind TER to ensure proper folding and biogenesis and not for use as a guide for RNA pseudouridylation [62]. Although the *Tetrahymena* telomerase holoenzyme exists as a monomer, whether human telomerase is a monomer or dimer is still debated [17,19].

Structural studies of human telomerase are significantly more challenging than *Tetrahymena* telomerase due to its even lower level of cellular expression and cell cycle regulation of the subunit composition, making homogeneous purification difficult [62]. Sauerwald and co-workers [20] overcame the problem of low *de novo* concentration by purifying telomerase from human embryonic kidney 293T cancer cells transiently transfected with plasmids containing the genes for TERT and TER [63]. Mass spectrometry of the purified sample detected Dyskerin and Nop10 in addition to the overexpressed TERT and TER [20].

The EM structure shows a bilobal dimer, with the TERT catalytic pockets separated by ~185 Å (Figure 3a) and seen in either an “open” or “closed” state, which is linked together by a flexible interface. To provide support that the dimer is the functional unit *in vivo*, the authors present evidence that both TERTs need to be active for catalytic activity *in vitro*. In other words, a single catalytically inactive TERT has a dominant-negative impact on the activity of the dimer [20]. The authors hypothesize that dimerization may allow telomerase to bind and elongate two G-overhangs on sister telomeres simultaneously. The structures of the monomers were reconstructed to 23 Å for the open state and 21 Å for the closed state by splitting the raw particle images and performing model-based angular 3D reconstruction from negative-stain EM [20]. The *Tribolium* TERT crystal structure was then fit into the periphery of the open monomer (Figure 3b). The location of the template RNA was deduced from visualization of colloidal gold-tagged DNA primer bound to the template RNA [20]. The authors also identify a continuous tubular density with a diameter of 25–30 Å opposite

to the proposed exit site of the telomere DNA, which they propose could be an RNA helix (Figure 3b circled).

The EM structures of the *Tetrahymena* telomerase holoenzyme and human telomerase monomer differ significantly (Figure 3b,c), which is not surprising given the difference in holoenzyme components and the size of TER (451 nt in human *versus* 159 nt in *Tetrahymena*). Significantly, the ring-shaped EM density assigned to TERT shows very similar structural features in the two 3D reconstructions and each has the active sites facing in toward the rest of the EM density. The proposed RNA helix in the human telomerase structure is in a similar location to where the pseudoknot and TEN domain are modeled in the *Tetrahymena* telomerase structure. However, in human telomerase, there is no density for TER CR4/5, which is the functional equivalent of *Tetrahymena* TER Loop 4 and known to bind the TERT TRBD (Figure 3b,c arrows) [50]. It is possible that some components of human telomerase were missing due to over-expression of TERT and TER or disrupted during purification due to proteolysis or buffer conditions, and that consequent structural flexibility averaged out some elements such as CR4/5 during EM image processing. Similarly, the N-terminal domain of p65 is absent in some EM images of the *Tetrahymena* telomerase holoenzyme, but the CTD and TER Stem-Loop 4 are always seen [21].

## Crystal Structure of the TERT RNA Binding Domain (TRBD) from *Takifugu rubripes*, the Japanese Puffer Fish

The 2.4 Å crystal structure of the TRBD from the *Takifugu rubripes* fish (*Tr*TRBD) is the first domain of a vertebrate TERT solved to date (Figure 2c) [24]. The structure has mainly alpha helical topology similar to the *Tribolium castaneum* TRBD and the *Tetrahymena thermophila* TRBD (Figure 2c) [44,50]. The major differences are mainly at the boundaries between the TRBD and the reverse transcriptase (RT) domain and the N-terminal linker, which joins the TRBD to the TEN domain. The N-terminal linker harbors the vertebrate-specific RNA (VSR) binding motif and a newly discovered motif the authors coin “TFLY” after its conserved TxxFLY sequence (Figure 2c) [24]. Amino acid substitutions within the TFLY reduced TBE binding and also disrupted the activity and processivity of full-length *E. coli* expressed *Tr*TERT assembled with TER *in vitro* [24]. Substituting E515, which lies at the tip of the T-motif and points toward the active site of TERT, with alanine caused only a modest decrease in TBE binding but a significant disruption in activity, further supporting the importance of the T-CP pocket in telomerase activity [7]. Three conserved residues previously found to cross-link the TRBD [50] and TER CR4/5 of medaka fish (*Oryzias latipes*) are clustered on one side of the *Tr*TRBD (Figure 2c) [24], with W461 in a position corresponding to the TRBD-CTE boundary in *Tribolium* TERT, and agreeing with the hypothesis that P6.1 inserts between these two domains in the RNP. The high similarity between the TRBD from *Takifugu rubripes*, *Tetrahymena thermophila*, and *Tribolium Castaneum* is consistent with the importance of this domain for TER binding.

## *S. cerevisiae* H/ACA RNP Structures

Vertebrate H/ACA RNPs consist of dyskerin (Cbf5 in yeasts), Nhp2, Nop10, Gar1, and a site-specific guide RNA containing the conserved H-box and ACA sequence motifs (Figure 4a) [61,64]. Though most H/ACA RNPs function in template-guided pseudouridylation, an H/ACA scaRNP domain is part of the vertebrate telomerase holoenzyme [16,65,66]. Mutations in dyskerin—as well as in other H/ACA RNP subunits and telomerase specific—proteins can lead to improper telomere maintenance and genetic diseases including dyskeratosis congenita (DC), aplastic anemia, and pulmonary fibrosis [67]. Structures of a single H/ACA hairpin in complex with archaeal H/ACA RNP proteins have been previously reported (see [61,68–70] for reviews). Recently, several structures of eukaryotic H/ACA

proteins from *S. cerevisiae* were reported [26–29]. These are the first structures of Nhp2 [26], which is replaced by L7Ae in archaea, the ternary complex of Cbf5-Nop10-Gar1 [28], and the H/ACA RNP assembly protein Shq1 C-terminal SSD domain both free [27] and in complex with Cbf5-Nop10-Gar1 [29]. *S. cerevisiae* telomerase RNA does not contain an H/ACA scaRNA domain so we do not review these in detail here. These new structures will allow for more accurate modeling of the Dyskerin-Nop10-Nhp2-Gar1 complex on the TER H/ACA scaRNA domain and of known disease-related mutations in the N- and C-terminal extensions of Cbf5, absent in the H/ACA RNP structure from archaea [71].

## Telomerase RNA Pseudoknots

Previous structural studies revealed an essential triple helix in the pseudoknot of human TER [72,73], and sequence analysis, mutatgenesis, and modeling has indicated that the triple helix is a conserved element required for telomerase function [72–76]. The NMR solution structure of the *Kluyveromyces lactis* pseudoknot was recently reported, revealing that despite significant sequence variation, it has a remarkably similar overall fold to the human pseudoknot (Figure 4b) [25]. Both pseudoknots contain stacked stems and a stabilizing triple helix. Surprisingly, the *K. lactis* pseudoknot contains 3 bulged nucleotides between successive Watson-Crick base pairs in the triple helix region and 6 consecutive major groove triples, 5 U-A-U and a single C-G-C, which span 11 base pairs of stem 2 (Figure 4b). Based on this structure, the authors also propose a model for the triple interactions in the *S. cerevisiae* TER pseudoknot (Figure 4c) that contains additional interactions not previously predicted [76]. A single-molecule fluorescence resonance energy transfer (smFRET) study of the isolated human TER t/PK domain, lacking the core enclosing helix P1, showed that it samples different conformations under different conditions, but the pseudoknot fold is stabilized by $Mg^{2+}$ ions [51]. The *Tetrahymena* TER pseudoknot, on the other hand, is less stable, and based on smFRET and MD studies only appears to fold properly in the context of full-length TER in the presence of telomerase protein components [52,77].

The divergent size and sequence of TER has made it difficult to identify and characterize it in a number of species. Recently, the first invertebrate TER, from *S. purpuratus* [78], as well as a number of fungal TERs, including *A. oryzae* whose secondary structure was confirmed by phylogenetic analysis [10,79] were identified. Predicted secondary structures of these TERs indicate that the conserved template/pseudoknot core domain, including a triple helix in the pseudoknot (Figure 4c), and a distal stem terminus element are present in these organisms.

## Future Prospects

Significant progress has been made in the past two years on the structural biology of telomerase. These studies were greatly facilitated by the combined use of NMR, X-ray crystallography, and electron microscopy, as well as other biophysical techniques such as single-molecule FRET. Significant challenges remain in getting ordered and homogeneous holoenzymes and protein-RNA complexes for structural studies. Future high resolution structures will provide unprecedented opportunity to study the mechanism of action and for structure based drug design of this remarkable enzyme.

## Acknowledgments

This work was supported by NIH grant GM48123 and NSF grant MCB1022379 to J.F. and a Ruth L. Kirschstein NRSA postdoctoral fellowship GM101874 to E.J.M.

## References


1. Nandakumar J, Cech TR. Finding the end: recruitment of telomerase to telomeres. Nat Rev Mol Cell Biol. 2013; 14:69–82. [PubMed: 23299958]
2. Hayflick L, Moorhead P. The serial cultivation of human diploid cell strains. Exp Cell Res. 1961; 25:585–621. [PubMed: 13905658]
3. Bernardes de Jesus B, Blasco MA. Telomerase at the intersection of cancer and aging. Trends Genet. 2013; 29:513–520. [PubMed: 23876621]
4. Buseman CM, Wright WE, Shay JW. Is telomerase a viable target in cancer? Mutat Res. 2012; 730:90–97. [PubMed: 21802433]
5. Mason M, Schuller A, Skordalakes E. Telomerase structure function. Curr Opin Struct Biol. 2011; 21:92–100. [PubMed: 21168327]
6. Jacobs SA, Podell ER, Cech TR. Crystal structure of the essential N-terminal domain of telomerase reverse transcriptase. Nat Struct Mol Biol. 2006; 13:218–225. [PubMed: 16462747]
7. Rouda S, Skordalakes E. Structure of the RNA-binding domain of telomerase: implications for RNA recognition and binding. Structure. 2007; 15:1403–1412. [PubMed: 17997966]
8. Greider CW, Blackburn EH. A telomeric sequence in the RNA of Tetrahymena telomerase required for telomere repeat synthesis. Nature. 1989; 337:331–337. [PubMed: 2463488]
9. Kachouri-Lafond R, Dujon B, Gilson E, Westhof E, Fairhead C, Teixeira MT. Large telomerase RNA, telomere length heterogeneity and escape from senescence in Candida glabrata. FEBS Lett. 2009; 583:3605–3610. [PubMed: 19840797]
10. Qi X, Li Y, Honda S, Hoffmann S, Marz M, Mosig A, Podlevsky JD, Stadler PF, Selker EU, Chen JJ-L. The common ancestral core of vertebrate and fungal telomerase RNAs. Nucleic Acids Res. 2013; 41:450–462. [PubMed: 23093598]
11. Lin J, Ly H, Hussain A, Abraham M, Pearl S, Tzfati Y, Parslow TG, Blackburn EH. A universal telomerase RNA core structure includes structured motifs required for binding the telomerase reverse transcriptase protein. Proc Natl Acad Sci U S A. 2004; 101:14713–14718. [PubMed: 15371596]
12. Miller MC, Collins K. Telomerase recognizes its template by using an adjacent RNA motif. Proc Natl Acad Sci U S A. 2002; 99:6585–6590. [PubMed: 11997465]
13. Mefford MA, Rafiq Q, Zappulla DC. RNA connectivity requirements between conserved elements in the core of the yeast telomerase RNP. EMBO J. 2013; 32:2980–2993. [PubMed: 24129512]
14. Livengood AJ, Zaug AJ, Cech TR. Essential regions of Saccharomyces cerevisiae telomerase RNA: separate elements for Est1p and Est2p interaction. Mol Cell Biol. 2002; 22:2366–2374. [PubMed: 11884619]
15. Laterreur N, Eschbach SH, Lafontaine DA, Wellinger RJ. A new telomerase RNA element that is critical for telomere elongation. Nucleic Acids Res. 2013; 41:7713–7724. [PubMed: 23783570]
16. Mitchell JR, Cheng J, Collins K. A box H/ACA small nucleolar RNA-like domain at the human telomerase RNA 3′ end. Mol Cell Biol. 1999; 19:567–576. [PubMed: 9858580]
17. Egan ED, Collins K. Specificity and stoichiometry of subunit interactions in the human telomerase holoenzyme assembled in vivo. Mol Cell Biol. 2010; 30:2775–2786. [PubMed: 20351177]
18. Theimer CA, Feigon J. Structure and function of telomerase RNA. Curr Opin Struct Biol. 2006; 16:307–318. [PubMed: 16713250]
19. Sekaran VG, Soares J, Jarstfer MB. Structures of telomerase subunits provide functional insights. Biochim Biophys Acta. 2010; 1804:1190–1201. [PubMed: 19665593]
20. Sauerwald A, Sandin S, Cristofari G, Scheres SHW, Lingner J, Rhodes D. Structure of active dimeric human telomerase. Nat Struct Mol Biol. 2013; 20:454–460. [PubMed: 23474713]
21. Jiang J, Miracco EJ, Hong K, Eckert B, Chan H, Cash DD, Min B, Zhou ZH, Collins K, Feigon J. The architecture of Tetrahymena telomerase holoenzyme. Nature. 2013; 496:187–192. [PubMed: 23552895]
22. Singh M, Wang Z, Koo B-K, Patel A, Cascio D, Collins K, Feigon J. Structural basis for telomerase RNA recognition and RNP assembly by the holoenzyme La family protein p65. Mol Cell. 2012; 47:16–26. [PubMed: 22705372]

23. Zeng Z, Min B, Huang J, Hong K, Yang Y, Collins K, Lei M. Structural basis for Tetrahymena telomerase processivity factor Teb1 binding to single-stranded telomeric-repeat DNA. Proc Natl Acad Sci U S A. 2011; 108:20357–20361. [PubMed: 22143754]
24. Harkisheimer M, Mason M, Shuvaeva E, Skordalakes E. A Motif in the Vertebrate Telomerase N-Terminal Linker of TERT Contributes to RNA Binding and Telomerase Activity and Processivity. Structure. 2013; 21:1870–1878. [PubMed: 24055314]
25. Cash DD, Cohen-Zontag O, Kim N-K, Shefer K, Brown Y, Ulyanov NB, Tzfati Y, Feigon J. Pyrimidine motif triple helix in the Kluyveromyces lactis telomerase RNA pseudoknot is essential for function in vivo. Proc Natl Acad Sci U S A. 2013; 110:10970–10975. [PubMed: 23776224]
26. Koo B-K, Park C-J, Fernandez CF, Chim N, Ding Y, Chanfreau G, Feigon J. Structure of H/ACA RNP protein Nhp2p reveals cis/trans isomerization of a conserved proline at the RNA and Nop10 binding interface. J Mol Biol. 2011; 411:927–942. [PubMed: 21708174]
27. Walbott H, Machado-Pinilla R, Liger D, Blaud M, Rety S, Grozdanov PN, Godin K, van Tilbeurgh H, Varani G, Meier UT, et al. The H/ACA RNP assembly factor SHQ1 functions as an RNA mimic. Genes Dev. 2011; 25:2398–2408. [PubMed: 22085966]
28. Li S, Duan J, Li D, Yang B, Dong M, Ye K. Reconstitution and structural analysis of the yeast box H/ACA RNA-guided pseudouridine synthase. Genes Dev. 2011; 25:2409–2421. [PubMed: 22085967]
29. Li S, Duan J, Li D, Ma S, Ye K. Structure of the Shq1-Cbf5-Nop10-Gar1 complex and implications for H/ACA RNP biogenesis and dyskeratosis congenita. EMBO J. 2011; 30:5010–5020. [PubMed: 22117216]
30. Blackburn EH, Gall JG. A tandemly repeated sequence at the termini of the extrachromosomal ribosomal RNA genes in Tetrahymena. J Mol Biol. 1978; 120:33–53. [PubMed: 642006]
31. Greider CW, Blackburn EH. Identification of a specific telomere terminal transferase activity in Tetrahymena extracts. Cell. 1985; 43:405–413. [PubMed: 3907856]
32. Blackburn E, Gilley D, Ware T, Bhattacharyya A, Kirk K, Wang H. Studying the telomerase RNA in Tetrahymena. Methods Cell Biol. 2000; 62:417–432. [PubMed: 10503207]
33. Witkin KL, Collins K. Holoenzyme proteins required for the physiological assembly and activity of telomerase. Genes Dev. 2004; 18:1107–1118. [PubMed: 15131081]
34. Witkin KL, Prathapam R, Collins K. Positive and negative regulation of Tetrahymena telomerase holoenzyme. Mol Cell Biol. 2007; 27:2074–2083. [PubMed: 17220281]
35. Min B, Collins K. An RPA-related sequence-specific DNA-binding subunit of telomerase holoenzyme is required for elongation processivity and telomere maintenance. Mol Cell. 2009; 36:609–619. [PubMed: 19941821]
36. Stone MD, Mihalusova M, O'connor CM, Prathapam R, Collins K, Zhuang X. Stepwise protein-mediated RNA folding directs assembly of telomerase ribonucleoprotein. Nature. 2007; 446:458–461. [PubMed: 17322903]
37. Berman AJ, Akiyama BM, Stone MD, Cech TR. The RNA accordion model for template positioning by telomerase RNA during telomeric DNA synthesis. Nat Struct Mol Biol. 2011; 18:1371–1375. [PubMed: 22101935]
38. Akiyama BM, Loper J, Najarro K, Stone MD. The C-terminal domain of Tetrahymena thermophila telomerase holoenzyme protein p65 induces multiple structural changes in telomerase RNA. RNA. 2012; 18:653–660. [PubMed: 22315458]
39. Min B, Collins K. Multiple mechanisms for elongation processivity within the reconstituted tetrahymena telomerase holoenzyme. J Biol Chem. 2010; 285:16434–16443. [PubMed: 20363756]
40. Henderson R. Avoiding the pitfalls of single particle cryo-electron microscopy: Einstein from noise. Proc Natl Acad Sci U S A. 2013; 110:18037–18041. [PubMed: 24106306]
41. Hong K, Upton H, Miracco EJ, Jiang J, Zhou ZH, Feigon J, Collins K. Tetrahymena Telomerase Holoenzyme Assembly, Activation, and Inhibition by Domains of the p50 Central Hub. Mol Cell Biol. 2013; 33:3962–3971. [PubMed: 23918804]
42. Cunningham DD, Collins K. Biological and biochemical functions of RNA in the tetrahymena telomerase holoenzyme. Mol Cell Biol. 2005; 25:4442–4454. [PubMed: 15899850]
43. Bryan TM, Goodrich KJ, Cech TR. Tetrahymena telomerase is active as a monomer. Mol Biol Cell. 2003; 14:4794–4804. [PubMed: 13679509]

44. Gillis AJ, Schuller AP, Skordalakes E. Structure of the Tribolium castaneum telomerase catalytic subunit TERT. Nature. 2008; 455:633–637. [PubMed: 18758444]
45. Mitchell M, Gillis A, Futahashi M, Fujiwara H, Skordalakes E. Structural basis for telomerase catalytic subunit TERT binding to RNA template and telomeric DNA. Nat Struct Mol Biol. 2010; 17:513–518. [PubMed: 20357774]
46. Leeper TC, Varani G. The structure of an enzyme-activating fragment of human telomerase RNA. RNA. 2005; 11:394–403. [PubMed: 15703438]
47. Richards RJ, Theimer CA, Finger LD, Feigon J. Structure of the Tetrahymena thermophila telomerase RNA helix II template boundary element. Nucleic Acids Res. 2006; 34:816–825. [PubMed: 16452301]
48. Bryan TM, Goodrich KJ, Cech TR. Telomerase RNA bound by protein motifs specific to telomerase reverse transcriptase. Mol Cell. 2000; 6:493–499. [PubMed: 10983995]
49. O'Connor CM, Lai CK, Collins K. Two purified domains of telomerase reverse transcriptase reconstitute sequence-specific interactions with RNA. J Biol Chem. 2005; 280:17533–17539. [PubMed: 15731105]
50. Bley CJ, Qi X, Rand DP, Borges CR, Nelson RW, Chen JJ-L. RNA-protein binding interface in the telomerase ribonucleoprotein. Proc Natl Acad Sci U S A. 2011; 108:20333–20338. [PubMed: 22123986]
51. Hengesbach M, Kim N-K, Feigon J, Stone MD. Single-molecule FRET reveals the folding dynamics of the human telomerase RNA pseudoknot domain. Angew Chem Int Ed Engl. 2012; 51:5876–5879. [PubMed: 22544760]
52. Mihalusova M, Wu JY, Zhuang X. Functional importance of telomerase pseudoknot revealed by single-molecule analysis. Proc Natl Acad Sci U S A. 2011; 108:20339–20344. [PubMed: 21571642]
53. Wu JY, Stone MD, Zhuang X. A single-molecule assay for telomerase structure-function analysis. Nucleic Acids Res. 2010; 38:e16. [PubMed: 19920121]
54. Steczkiewicz K, Zimmermann MT, Kurcinski M, Lewis BA, Dobbs D, Kloczkowski A, Jernigan RL, Kolinski A, Ginalski K. Human telomerase model shows the role of the TEN domain in advancing the double helix for the next polymerization step. Proc Natl Acad Sci U S A. 2011; 108:9443–9448. [PubMed: 21606328]
55. Bousquet-Antonelli C, Deragon J-M. A comprehensive analysis of the La-motif protein superfamily. RNA. 2009; 15:750–764. [PubMed: 19299548]
56. O'Connor CM, Collins K. A novel RNA binding domain in tetrahymena telomerase p65 initiates hierarchical assembly of telomerase holoenzyme. Mol Cell Biol. 2006; 26:2029–2036. [PubMed: 16507983]
57. Berman AJ, Gooding AR, Cech TR. Tetrahymena telomerase protein p65 induces conformational changes throughout telomerase RNA (TER) and rescues telomerase reverse transcriptase and TER assembly mutants. Mol Cell Biol. 2010; 30:4965–4976. [PubMed: 20713447]
58. Singh M, Choi CP, Feigon J. xRRM: A new class of RRM found in the telomerase La family protein p65. RNA Biol. 2013; 10
59. Fan J, Pavletich NP. Structure and conformational change of a replication protein A heterotrimer bound to ssDNA. Genes Dev. 2012; 26:2337–2347. [PubMed: 23070815]
60. Lei M, Podell ER, Cech TR. Structure of human POT1 bound to telomeric single-stranded DNA provides a model for chromosome end-protection. Nat Struct Mol Biol. 2004; 11:1223–1229. [PubMed: 15558049]
61. Hamma T, Ferré-D'Amare AR. The box H/ACA ribonucleoprotein complex: interplay of RNA and protein structures in post-transcriptional RNA modification. J Biol Chem. 2010; 285:805–809. [PubMed: 19917616]
62. Egan ED, Collins K. Biogenesis of telomerase ribonucleoproteins. RNA. 2012; 18:1747–1759. [PubMed: 22875809]
63. Cristofari G, Lingner J. Telomere length homeostasis requires that telomerase levels are limiting. EMBO J. 2006; 25:565–574. [PubMed: 16424902]
64. Egan ED, Collins K. An enhanced H/ACA RNP assembly mechanism for human telomerase RNA. Mol Cell Biol. 2012; 32:2428–2439. [PubMed: 22527283]

65. Sexton AN, Youmans DT, Collins K. Specificity requirements for human telomere protein interaction with telomerase holoenzyme. J Biol Chem. 2012; 287:34455–34464. [PubMed: 22893708]
66. Machado-Pinilla R, Liger D, Leulliot N, Meier UT. Mechanism of the AAA+ ATPases pontin and reptin in the biogenesis of H/ACA RNPs. RNA. 2012; 18:1833–1845. [PubMed: 22923768]
67. Batista LF, Artandi SE. Understanding telomere diseases through analysis of patient-derived iPS cells. Curr Opin Genet Dev. 2013; 23:526–533. [PubMed: 23993228]
68. Ye K. H/ACA guide RNAs, proteins and complexes. Curr Opin Struct Biol. 2007; 17:287–292. [PubMed: 17574834]
69. Li H. Unveiling substrate RNA binding to H/ACA RNPs: one side fits all. Curr Opin Struct Biol. 2008; 18:78–85. [PubMed: 18178425]
70. Kiss T, Fayet-Lebaron E, Jády BE. Box H/ACA small ribonucleoproteins. Mol Cell. 2010; 37:597–606. [PubMed: 20227365]
71. Li L, Ye K. Crystal structure of an H/ACA box ribonucleoprotein particle. Nature. 2006; 443:302–307. [PubMed: 16943774]
72. Theimer CA, Blois CA, Feigon J. Structure of the human telomerase RNA pseudoknot reveals conserved tertiary interactions essential for function. Mol Cell. 2005; 17:671–682. [PubMed: 15749017]
73. Kim N-K, Zhang Q, Zhou J, Theimer CA, Peterson RD, Feigon J. Solution structure and dynamics of the wild-type pseudoknot of human telomerase RNA. J Mol Biol. 2008; 384:1249–1261. [PubMed: 18950640]
74. Shefer K, Brown Y, Gorkovoy V, Nussbaum T, Ulyanov NB, Tzfati Y. A triple helix within a pseudoknot is a conserved and essential element of telomerase RNA. Mol Cell Biol. 2007; 27:2130–2143. [PubMed: 17210648]
75. Ulyanov NB, Shefer K, James TL, Tzfati Y. Pseudoknot structures with conserved base triples in telomerase RNAs of ciliates. Nucleic Acids Res. 2007; 35:6150–6160. [PubMed: 17827211]
76. Qiao F, Cech TR. Triple-helix structure in telomerase RNA contributes to catalysis. Nat Struct Mol Biol. 2008; 15:634–640. [PubMed: 18500353]
77. Cole DI, Legassie JD, Bonifacio LN, Sekaran VG, Ding F, Dokholyan NV, Jarstfer MB. New models of Tetrahymena telomerase RNA from experimentally derived constraints and modeling. J Am Chem Soc. 2012; 134:20070–20080. [PubMed: 23163801]
78. Li Y, Podlevsky JD, Marz M, Qi X, Hoffmann S, Stadler PF, Chen JJ-L. Identification of purple sea urchin telomerase RNA using a next-generation sequencing based approach. RNA. 2013; 19:852–860. [PubMed: 23584428]
79. Kuprys PV, Davis SM, Hauer TM, Meltser M, Tzfati Y, Kirk KE. Identification of telomerase RNAs from filamentous fungi reveals conservation with vertebrates and yeasts. PLoS One. 2013; 8:e58661. [PubMed: 23555591]
80. Richards RJ, Wu H, Trantirek L, O'Connor CM, Collins K, Feigon J. Structural study of elements of Tetrahymena telomerase RNA stem-loop IV domain important for function. RNA. 2006; 12:1475–1485. [PubMed: 16809815]

## Highlights

- Electron microscopy structure and subunit architecture of *Tetrahymena* telomerase holoenzyme
- The electron microscopy structure of human telomerase
- First structures of *Tetrahymena* telomerase proteins outside of TERT
- The RNA pseudoknot structure from *K. lactis* TER

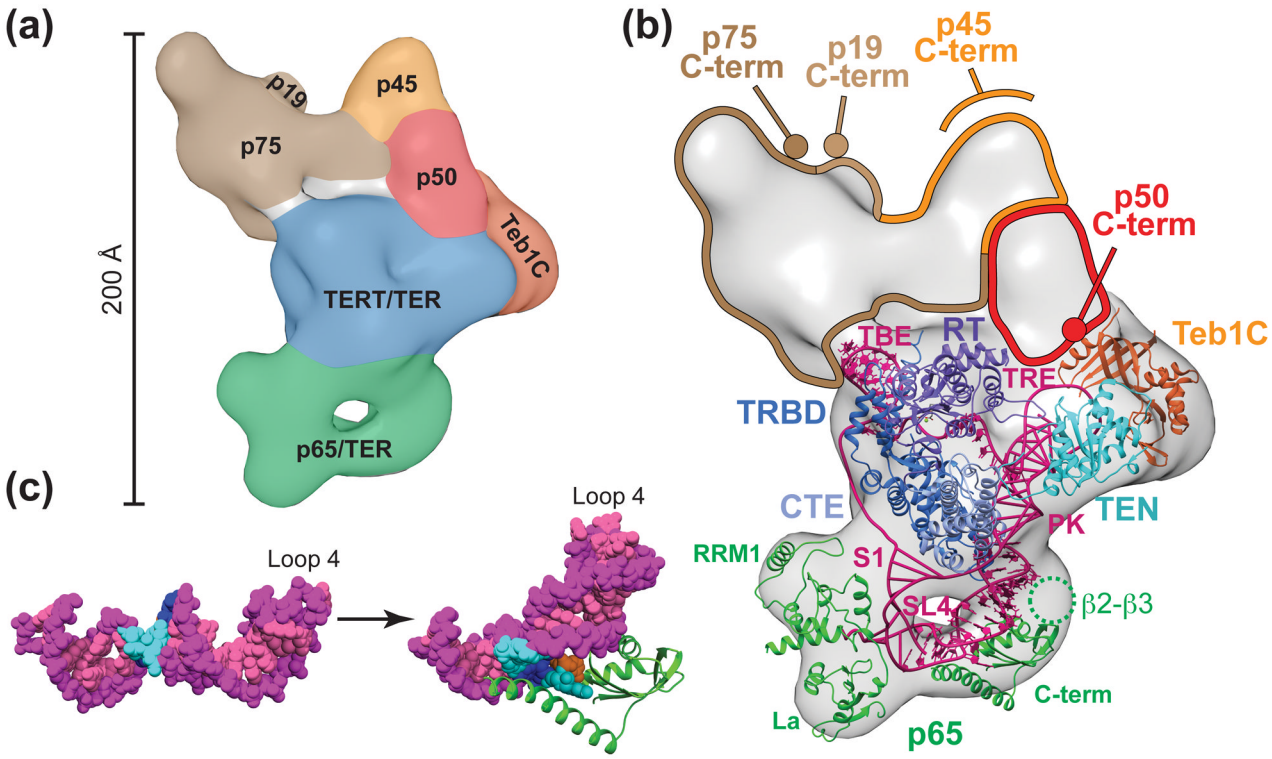


**Figure 1. Subunit architecture and model of the catalytic core in the *Tetrahymena* EM structure**

**(a)** The 25 Å EM model of the *Tetrahymena* telomerase holoenzyme with locations and known boundaries of subunits colored in. **(b)** Model of the *Tetrahymena* telomerase holoenzyme with the complete TERT-TER-p65 RNP catalytic core plus Teb1C (PDB ID: 3U50) modeled into the EM map. Modeled domains of TER are represented by tube and ladder and NMR structures are shown with atoms. **(c)** NMR solution structure of *Tetrahymena* TER Stem 4 (PDB ID: 2FEY) [80] and Loop 4 (PDB ID: 2M21) and crystal structure of *Tetrahymena* p65 xRRM bound to Stem 4 (PDB ID: 4ERD) with Loop 4 modeled.

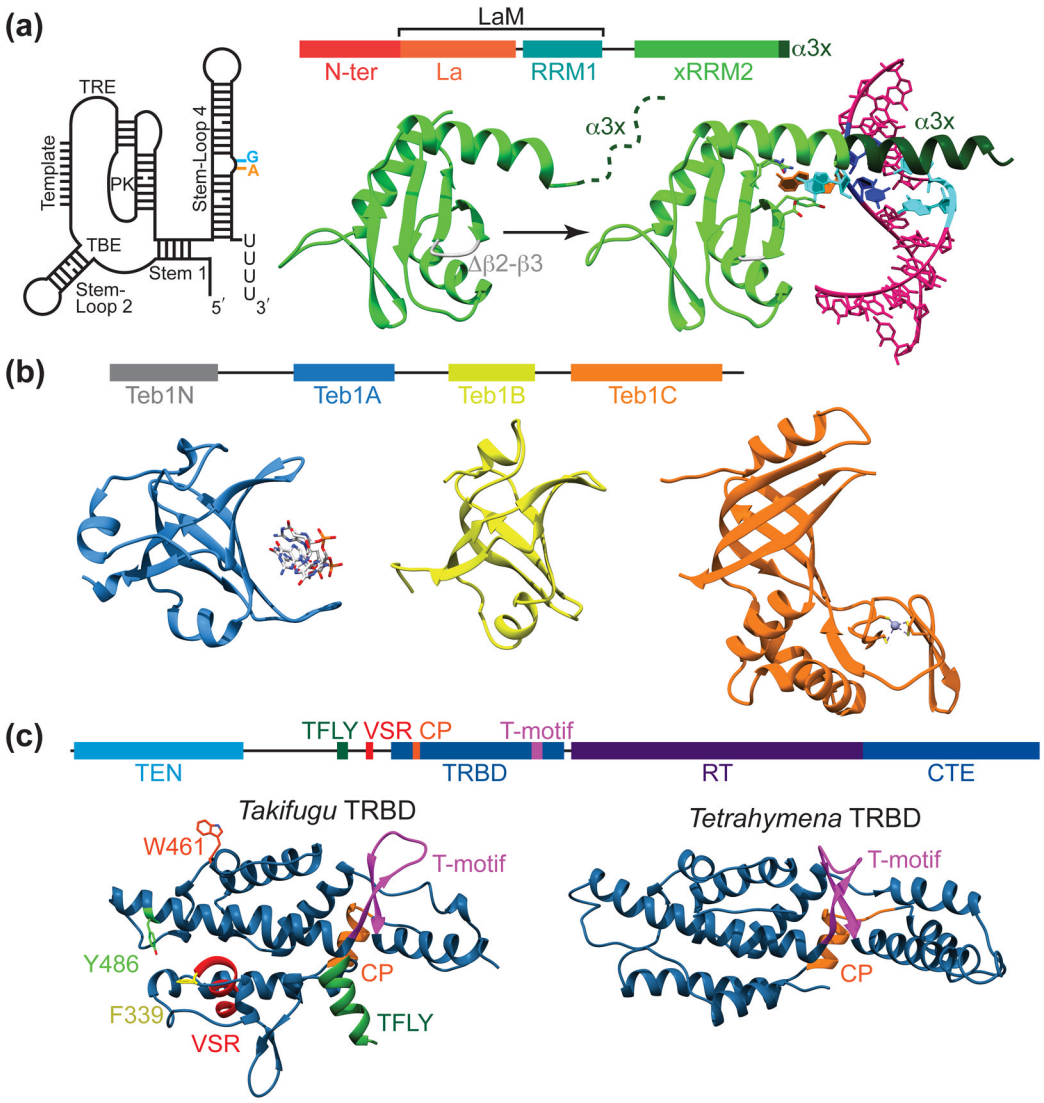


**Figure 2. Crystal structures of *Tetrahymena* p65 xRRM, Teb1 A, B, and C, and *Takifugu rubripes* TRBD**

**(a)** p65-TER interactions. At top, schematic of domain structure of p65. (left) Secondary structure schematic of *Tetrahymena* TER with Stem-Loop 4 bulge guanosine (cyan) adenosine (orange) colored (center) p65 xRRM (green) free (PDB ID: 4EYT) and in complex with Stem 4 (PDB ID: 4ERD). The unstructured α3x in the free xRRM is shown as a dashed dark green line, and is structured in the complex with Stem 4 (magenta). **(b)** Teb1 domains and interaction with telomere DNA. At top, schematic of domain structure of Teb1. Crystal structures of (left) Teb1A from Teb1AB co-crystal structure (blue) with telomeric DNA (grey) (PDB ID: 3U58), (middle) Teb1B (yellow) (PDB ID: 3U4Z), and (right) Teb1C (orange) with zinc (silver) coordinated by four cysteines of the zinc ribbon (PDB ID: 3U50). **(c)** *Takifugu rubripes* TERT TRBD structure. At top, schematic of domain structure of *Takifugu rubripes* TERT. (left)*Takifugu rubripes* (PDB ID: 4LMO) and (right) *Tetrahymena* TRBD (PDB ID: 2R4G) crystal structures. T-motif (magenta) and CP (orange) form the T-CP pocket, which is elongated in the *Takifugu rubripes* TRBD by the TFLY (green) motif. Vertebrate-specific RNA binding motif (red) and homologous UV active residues (orange, green, and yellow) are all located in a similar location.

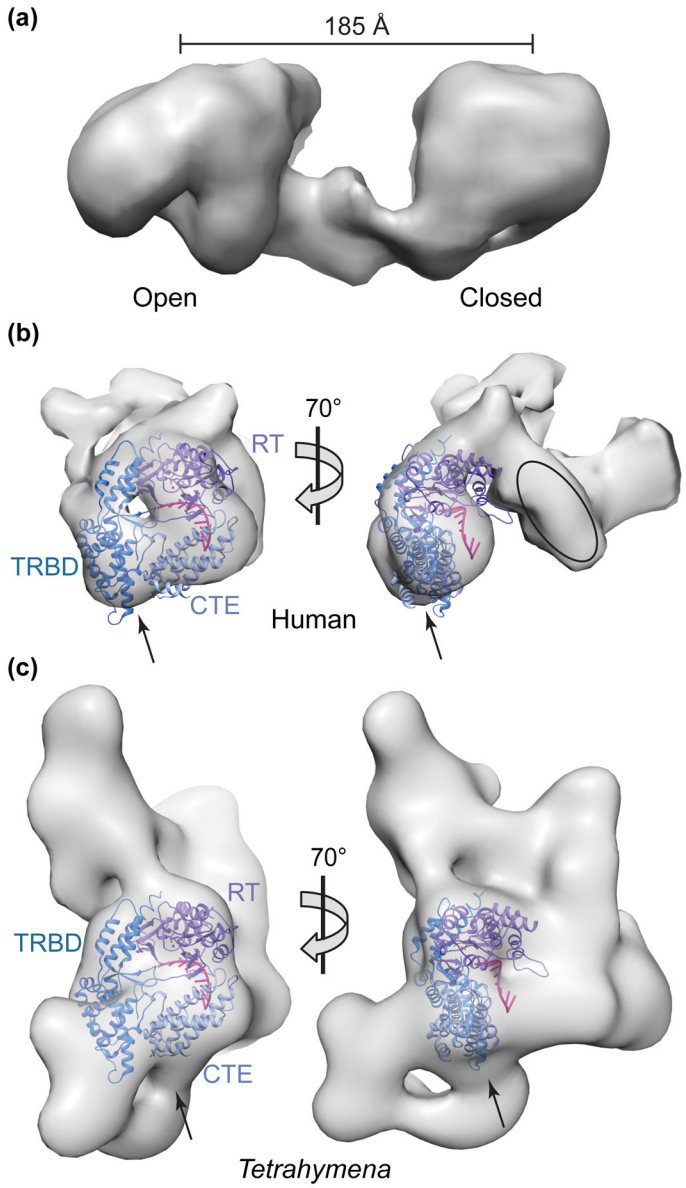


**Figure 3. EM structures of *Tetrahymena* telomerase holoenzyme and human telomerase dimer**

**(a)** EM structure of bilobal human telomerase dimer (EMDB: 2310). **(b)** and **(c)** EM structures of the "open" (EMDB: 2311) monomer of human telomerase dimer **b** and the *Tetrahymena* telomerase holoenzyme (EMDB: 5804) (**c**) with the TRBD, RT, and CTE of TERT and the template of TER modeled in. Proposed region of dsRNA in **b** is indicated with oval outline. The structures from *Tetrahymena* and human are shown with TERT (PDB ID: 3KYL) in the same orientation for comparison. The arrows point to the putative binding site of TER CR4/5 in human telomerase **b** and the modeled binding site of TER Stem 4 in the *Tetrahymena* telomerase holoenzyme **c**.

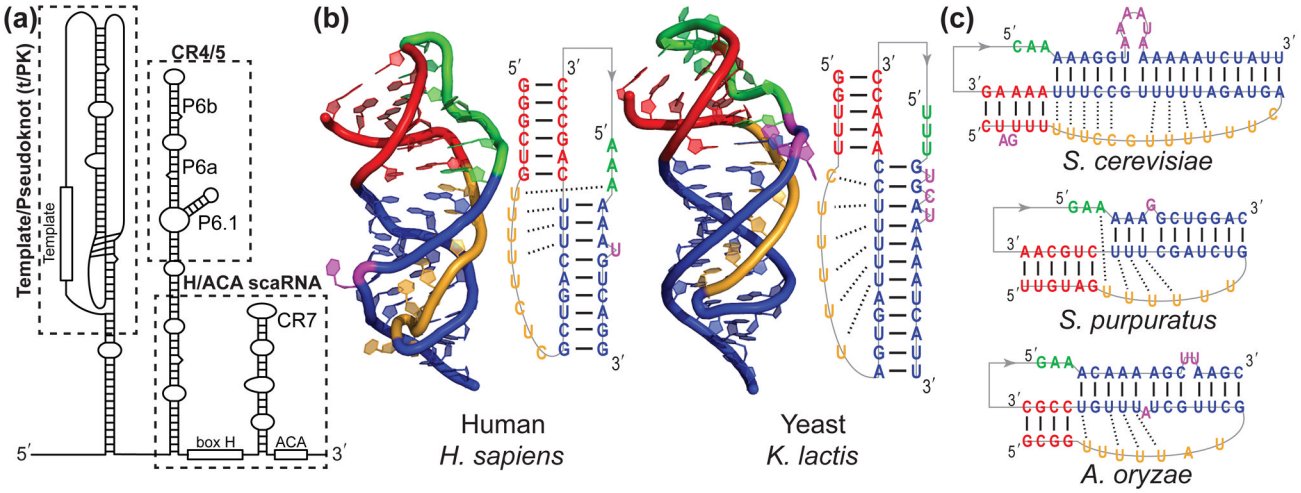


**Figure 4. Solution structures of telomerase pseudoknots**

**(a)** Secondary structure schematic of human TER with t/PK, CR4/5, and the H/ACA scaRNA motifs boxed. **(b)** Secondary structure schematic and NMR solution structure of the human P2b-P3 pseudoknot (left) (PDB ID: 1YMO) and *K. lactis* (right) (PDB ID: 2M8K). **(c)** Proposed pseudoknot secondary structure from (top) *S. cerevisiae* (budding yeast) [25], (middle) *S. purpuratus* (purple sea urchin) [78], and *A. oryzae* (filamentous fungi) [79].